 doi:10.20944/preprints202104.0588.v2

Predicting citywide distribution of air pollution using mobile monitoring and three-dimensional urban structure

Lucas E. Cummings*[1], Justin D. Stewart*[1,2], Peleg Kremer[1], Kabindra.M. Shakya[1]

*These authors contributed to this work equally
[1] Department of Geography and the Environment, Villanova University, Pennsylvania, USA
[2] Department of Ecological Science, Vrije Universiteit Amsterdam, 1081 HV Amsterdam, The Netherlands

Abstract

Understanding relationships between urban structure patterns and air pollutants is key to sustainable urban planning and development. This study employed mobile monitoring of PM2.5 and BC across ~480 Kilometers in Philadelphia, USA during summer 2019. We apply the 3D Structure of Urban Landscapes (STURLA) classification to examine relationships between urban structure and atmospheric pollution. We find that, while PM2.5 and BC vary by STURLA class, many of the differences in pollutant concentrations between classes are not significant. However, we also find that the proportions in which STURLA components are present throughout the urban landscape can be used to predict urban air pollution. Among frequently sampled STURLA classes, gpl hosted the highest PM2.5 concentrations on average (16.60 ± 4.29 µg/m3), while tgbwp hosted the highest BC concentrations (2.31 ± 1.94 µg/m3). Furthermore, STURLA combined with machine learning modeling was able to correlate PM2.5 (R2= 0.68, RMSE 2.82 µg/m3) and BC (R2 = 0.64, RMSE 0.75 µg/m3) concentrations with the composition of the urban landscape and predict concentrations where sampling did not take place. These results demonstrate the efficacy of the STURLA methodology in modeling relationships between air pollution and urban structure patterns.

Significance Statement

This study is the first to use the Structure of Urban Landscapes (STURLA) methodology in the context of air pollution modeling to examine relationships between air pollution and urban structure. The study also utilizes big data collected on a large spatial scale (483 km throughout Philadelphia) through a mobile monitoring method, which is a relatively

 doi:10.20944/preprints202104.0588.v2

new and accessible way to measure pollutant concentrations while providing high levels of spatial and temporal resolution.

Main Text

Introduction

Population growth in urban areas is increasing rapidly; the United Nations projects that 68% of the world's population will live in urban areas by 2050 (UN DESA, 2018). As urban areas expand, a larger proportion of the global population will be exposed to increasingly high and potentially harmful levels of air pollution. At present, 9 out of 10 people regularly breathe air containing unsafe level of air pollutants (WHO, 2018), and approximately 3.7 million premature deaths worldwide can be attributed to elevated air pollutant concentrations each year (Cohen et al., 2017). Elevated levels of air pollutants disproportionately impact people based on race, (Perlin et al. 1999; Gray et al. 2013), gender and sexual orientation (Collins et al., 2017a; Collins et al., 2017b) and socioeconomic status (Perlin et al. 1999; Zhou et al. 2011; Gray et al. 2013). To ensure that air quality management is equitable and protects the health of urban populations, it is crucial that we understand how air pollutants interact with the urban environment.

Particulate matter (PM) has been linked to negative health outcomes, including asthma (Halonen et al., 2008; Anenberg et al. 2018), lung cancer (Hamra et al. 2014; Pope et al. 2002), DNA alteration (Sørensen et al. 2003; Shi et al., 2019; Baccarelli et al., 2009), and disrupted immune function (Zelikoff et al., 2008; Honda et al. 2017). Polluted airs also host potentially pathogenic bacteria (Stewart et al., 2020; Liu et al., 2018) and viruses (Zhu et al., 2020) that may cause disease and aggravate pre-existing conditions. Fine particulate matter ($PM_{2.5}$) is of significant concern due to its abundance in urban atmospheres, and subsequent potential to cause respiratory and cardiovascular damage (Dockery et al., 1993; Paul et al., 2019; Rabinovitch et al., 2006; Shakya et al., 2016). Black carbon (BC), a subset of $PM_{2.5}$, is generated through incomplete combustion of fossil fuels and is particularly prevalent in urban areas. Unlike $PM_{2.5,}$ almost all of BC originates from anthropogenic sources, with biomass fires being the only natural source of BC (Hitzenberger & Tohno, 2001); as such, BC is commonly used as an indicator of anthropogenic influence on ambient air pollution (Cyrys et al., 2003; Targino et al., 2016).

Studies of urban air pollution have established relationships between landcover, urban structure, and ambient air pollution (Eeftens et al. 2012; Yuan et al. 2019). In urban areas such as Philadelphia, particulate matter concentrations vary across neighborhoods as a result of differences in open space and land structure (Shakya et al., 2019). The organization and height of buildings, barriers and other structures in an urban environment can influence air flow, which in turn impacts local pollutant dispersal (Baldauf et al., 2016; Gallagher et al., 2015; Ng & Chau, 2013). Though many urban areas are characterized by dense built environment, different types of urban green space (e.g. urban forest, parks, gardens, and private yards) are an integral part of the urban landscape. Over the last few decades, cities are increasingly adopting strategies such as urban greening to counteract environmental degradation and enhance human wellbeing. However, these strategies and their efficacy in mitigating urban air pollution are still unclear (Nemitz et al., 2020). While vegetation such as trees and grasses have been shown to reduce air pollution by facilitating pollutant deposition and uptake of

Preprints (www.preprints.org) | NOT PEER-REVIEWED | Posted: 5 May 2021 doi:10.20944/preprints202104.0588.v2

particulate matter, they are also capable of causing an increase in local pollutant concentrations through biogenic emissions that serve to facilitate secondary aerosol formation and the inhibition of air flow (Brantley et al. 2014; Chen et al. 2016; Eisenman et al. 2019; Xing & Brimblecombe 2019).

Although it is becoming increasingly clear how individual components of urban environments influence air pollution, complex urban topologies make it difficult to understand how these individual components interact to influence air pollution at more localized scales. In urban environments, landcover and urban structure often change drastically over short distances (Cadenasso et al., 2007). While cities may contain common environmental features such as water and greenspace, differences in their organization have varied impacts on air quality. This further complicates efforts to generalize the impact that urban environments have on air pollution. Sustainable development is contingent on reproducible and scalable analyses with geographically meaningful units for urban planning. To this end, there have been efforts to streamline the characterization of cities at smaller scales. The Structure of Urban Landscape (STURLA) composite classification system allows for modeling of three-dimensional urban areas at fine spatial scales. STURLA does so by using fine-scale landcover and building height data to identify common compositions of urban environments (Hamstead et al., 2016). STURLA studies have linked urban landscape structure and land surface temperature (Hamstead et al., 2016; Kremer et al. 2018; Larondelle et al., 2014; Mitz et al., 2021), as well as the phylogenetic diversity of the atmospheric microbiome (Stewart et al. 2021). STURLA allows for meaningful classifications of urban structure and landcover, which have the potential to reshape our understanding of how the composition and spatial organization of urban environments influence environmental parameters. There have also been efforts to improve the accuracy of urban air pollution measurement, as variability in three-dimensional urban landscape composition can influence pollutant dispersal and affect concentrations at small scales (Abhijith & Gokhale, 2015; Gallagher et al. 2015; Hagler et. al, 2012). In recent years, mobile monitoring has been used study the spatiotemporal distribution of air pollutants in cities (Apte et al., 2017; deSouza et al., 2020; Deville Cavellin et al., 2016; Shakya et al., 2019; Sm et al., 2019; Targino et al., 2016; Van Poppel et al., 2013). An advantage of mobile monitoring is that it can collect data at finer spatial scales than is feasible with stationary monitoring (Shakya et al., 2019; Van den Bossche et al., 2015) and subsequent spatial predictions logically should be more accurate and meaningful. In this study, we use data collected through mobile monitoring to measure concentrations of particulate matter smaller than 2.5 μm ($PM_{2.5}$) and black carbon (BC) throughout the city of Philadelphia over the course of 12 days during the summer of 2019 (Cummings & Stewart et al., 2021). We use STURLA in conjunction with the collected air pollution data to analyze the urban structure-air pollution relationship across the city of Philadelphia.

Results

Variation in Landscape Structure with $PM_{2.5}$ and BC Concentrations Among STURLA Classes

Differences in both landscape composition and the measured pollutant concentrations they host are evident among the most sampled STURLA classes (Figure

Preprints (www.preprints.org) | NOT PEER-REVIEWED | Posted: 5 May 2021 doi:10.20944/preprints202104.0588.v2

2). Although a slightly different subset of cells was sampled for $PM_{2.5}$ and BC due to differences in temporal resolutions of sampling equipment (5 seconds for BC compared to 6 seconds for $PM_{2.5}$), differences in average STURLA class composition are minimal and did not influence clustering between classes. Daily means for $PM_{2.5}$ among STURLA classes range from 11.47 $\pm$ 1.89 µg/m^3 (*tgbplm*) to 16.60 $\pm$ 4.29 µg/m^3 µg/m^3 (*gpl*), while daily means for BC range from 1.25 $\pm$ 0.71 µg/m^3 (*tgbplm*) to 2.31 $\pm$ 1.94 µg/m^3 (*tgbwp*) (Figure 2). Permutational t-tests reveal that some of the differences in pollutant concentrations between STURLA classes are statistically significant ($p < 0.05$) (Figure A3). Class *gpl* demonstrated the most unique $PM_{2.5}$ signature, with daily mean $PM_{2.5}$ concentrations differing significantly from six classes: *tgp, tgplm, tgwp, tgpm, tgbplm,* and *tgplmh*. Class *tgbplm* presented the most distinct BC signature with the daily average BC concentration being significantly different from four other classes sampled: *tgplmh, gpl, tgbwp,* and *gp.* However, other STURLA classes did not have pollutant concentrations that were significantly different from other classes. More significant differences between classes were found with $PM_{2.5}$ concentrations (17) than with BC concentrations (9) (Figure A3).

Spatial Modeling of $PM_{2.5}$ and BC

Pavement was the most important variable in modeling $PM_{2.5}$, followed by high-rise, grass, trees, mid-rise, water, and low-rise (Figure 3A). In modeling BC, low-rise was the most important variable, followed by pavement, trees, grass, mid-rise, high-rise, and water (Figure 3C). In both models, bare soil did not contribute to predictions of pollutant concentrations (Figures 3A, 3C). Predictions varied by STURLA class. Philadelphia's most frequent class, *tgpl*, has a mean prediction of 13.71 µg/m^3; modeling overpredicted the average measured concentration of the class by 1.64 µg/m^3. STURLA classes *gbp, tgp,* and *gpl* are among the classes with the highest predicted concentrations, while *pm, tgwpl, gwp* had the lowest (Table A4). Variation in $PM_{2.5}$ concentrations across the city were largely explained by differences in sampled STURLA classes ($R^2 = 0.68$, RMSE 1.10 µg/m^3). $PM_{2.5}$ predictions (Figure 3B) ranged from 8.77 – 15.29 µg/m^3; actual $PM_{2.5}$ concentrations by class ranged from 5.40 – 22.21 µg/m^3. Differences between STURLA class composition were slightly less effective in explaining variation in BC concentrations ($R^2 = 0.64$, RMSE 0.91 µg/m^3). BC predictions by class were generally higher than measured concentrations and ranged from 1.26 µg/m^3 to 3.76 µg/m^3 (Figure 3D); actual concentrations by class ranged from 0.85 – 5.45 µg/m^3. BC predictions in *tgpl* hosted predicted BC values of 1.65 µg/m^3 and overpredicted measured BC in *tgpl* pixels by 0.07 µg/m^3. Classes with more internal class elements generally have lower predicted air pollution concentrations; while *tpl, tp,* and *twpm* have the highest BC predictions, *tgbph, tgplmh,* and *tgbplh* have the lowest.

$PM_{2.5}$ predictions by planning district ranged from 12.62 µg/m^3 – 13.74 µg/m^3; the highest predicted $PM_{2.5}$ concentrations are in the Upper Far Northeast and Lower Far Northeast planning districts, while the lowest predicted concentrations were found in the Central planning district (Table A5). 17 of 18 planning districts underpredicted measured $PM_{2.5}$ concentrations (Predicted $PM_{2.5}$ / Measured $PM_{2.5}$ ratio < 1), which ranged from 12.74 µg/m^3 – 14.11 µg/m^3 (Table A5). $PM_{2.5}$ modeling was the most accurate in the Lower South district (Figure A4B), with a difference of 0.02 µg/m^3 between predicted and measured concentrations, but least accurate in the South district, with a 0.38 µg/m^3 difference between predicted and measured concentrations. Overpredictions were less common than underpredictions by STURLA class $PM_{2.5}$ with ~44% STURLA classes

Preprints (www.preprints.org) | NOT PEER-REVIEWED | Posted: 5 May 2021 doi:10.20944/preprints202104.0588.v2

underestimating concentrations (Figure A4A). for Conversely, the model predicted higher than measured BC concentrations in most STURLA classes (Table A5, Figure A4C) found in all planning districts (Figure A4D). Predicted BC concentrations ranged from 1.54 μg/m^3 – 1.78 μg/m^3, while measured BC concentrations ranged from 1.49 μg/m^3 – 1.66 μg/m^3. BC predictions are highest in the Lower South district and lowest in the Central district. BC modeling was most effective in the Central, Lower Far Northeast, North, North Delaware, River Wards, and University Southwest planning districts, all of which have 0.05 μg/m^3 between predicted and measured values; in the Lower South district, the difference between predicted and measured BC concentrations is at its highest (0.12 μg/m^3).

Discussion

Variation in $PM_{2.5}$ and BC by STURLA Class

$PM_{2.5}$ and BC varied by STURLA class (Figure 2); while some classes, such as *gpl* and no class had $PM_{2.5}$ concentrations or BC concentrations that were significantly different from all commonly sampled classes (Figure A3). Among the 14 most sampled STURLA classes, we find that the classes containing mid-rise and high-rise buildings hosted lower concentrations of $PM_{2.5}$ and BC relative to other commonly sampled classes; the five classes containing the vertical built environment *m* or *h* (*tgplm, tgpm, tgplh, tgplmh,* and *tgbplm*) show the lowest average concentrations of $PM_{2.5}$ and BC (Figure 2). Four of these five classes (*tgpm, tgplh, tgplmh,* and *tgbplm*) also have the lowest daily variation in $PM_{2.5}$ concentrations, while all five have the lowest daily variation in BC concentrations (Figure 2). While greater proportion of highrise buildings (Aristodemou et al., 2018) generally host higher air pollution concentrations, the compositional nature of STURLA may be picking up broader patterns. These classes also host greenspace, which tend to have lower concentrations of air pollutants (Leung et al., 2011; Li et al., 2016). A holistic view of greenspace with tall buildings may represent vegetation mediated pollution removal as well as dispersal limitation. Buildings restrict air flow and pollutant dispersal, causing an increase in pollutant concentrations closer to the peak of the building while decreasing concentrations at the ground-level where sampling occurred (Aristodemou et al., 2018; Zhang et al., 2013). Likewise, potential sources of PM and BC may simply be less abundant and/or smaller in magnitude where these classes are found, despite PM concentrations typically being higher in areas with denser built environment (Zhou & Lin, 2019). It is worth noting that classes with *m* and *h* components were generally sampled less frequently, except for *tgplm,* because they are less prevalent in the city's landscape. Some classes, such as *tgplh* and *tgplmh,* were not sampled enough to be able to quantify variability in pollutant concentrations on some days (Figure 2). Smaller sample sizes may have been less effective at capturing the full range of pollutant concentrations for specific classes than larger sample sizes.

While classes such as *tgbplm, tgplm,* and *tgplh,* are compositionally similar and have similar concentrations of $PM_{2.5}$ and BC (Figure 2), others display pronounced differences in pollutant levels despite compositional similarities with other STURLA classes. Among the most sampled STURLA classes, *gpl* hosted the highest $PM_{2.5}$ concentrations and the third-highest BC concentrations. Class *gpl* is largely dominated by built environment, with roughly 89.9% of *gpl* cells characterized by pavement and low-rise buildings (Figure 2). In class *tgplmh,* the class most similar to *gpl* by STURLA

Preprints (www.preprints.org) | NOT PEER-REVIEWED | Posted: 5 May 2021 doi:10.20944/preprints202104.0588.v2

elements, we observe the second-lowest daily average $PM_{2.5}$ and BC concentrations throughout the sampling period. Conversely, class *gp*– also compositionally similar to *gpl* – hosted relatively high concentrations of $PM_{2.5}$ and BC just like *gpl*. in this class, we observe the third-highest daily average $PM_{2.5}$ concentration and second-highest daily average BC concentration. The differences in these classes may be explained by the differences in variety of urban landscape components present; *gp* and *gpl* classes lack the trees, mid-rise, and high-rise buildings that are present in the *tgplmh* class. Even though *gp* is considerably more vegetated than *tgplmh* (43.2% grass in *gp* vs. 17.8% trees/grass in *tgplmh*), class *gp* has pollutant concentrations that are closer to *gpl*, a class with 89.8% built environment. The high pollutant concentrations in *gp* and *gpl* suggest that grass does not facilitate a meaningful decrease in PM in urban environments, or at least in areas of the urban environment that consist mostly of built environment. Trees may be more effective at attenuating air pollution than grass; most classes containing trees, with the exception of *tgbwpl,* have lower concentrations of $PM_{2.5}$ and BC than *gp* and *gpl*. However, given the prevalence of classes with trees in Philadelphia, it is unclear whether it is the abundance of trees or the lack of built environment that contributes more to lower pollutant concentrations in these classes.

Spatial Prediction of Air Pollution

The STURLA classification was able to capture air pollution signatures and used to model spatial patterns despite heterogeneity in daily concentrations of PM and BC resulting from variation in potential sources of pollution (e.g. on highways, near parks, stalled in traffic). Modeling was generally accurate for both $PM_{2.5}$ and BC; the largest difference between predicted and measured concentrations among planning districts was 0.38 $\mu g/m^3$ for $PM_{2.5}$ and 0.12 $\mu g/m^3$ for BC (Table A5). Both models relied on the built environment to predict pollutant concentrations; pavement and high-rise were the most important STURLA components in modeling $PM_{2.5}$. Low-rise and pavement were the most important components in modeling BC. Pavement's importance in modeling the relationships between STURLA and PM is likely a function of the sampling design, which requires driving on roads throughout the sampling period, as well as the prevalence of pavement throughout Philadelphia. This also become apparent when model error is mapped where greenspace, such as Fairmount Park, are difficult to accurately predict. As measuring directly in greenspace without pavement was not possible by car, we underestimate the contribution of trees and grass to air pollution attenuation (Nowak et al., 2006).

Vehicular emissions are a major contributor to PM emissions on roads (Cheng & Li, 2010), and developed areas in the urban environment are often in close proximity to facilities that generate PM pollution. The importance of low-rise buildings in BC modeling and the importance of high-rise buildings in $PM_{2.5}$ monitoring highlight the potential for buildings to influence pollutant concentrations. These buildings are not only positively associated with $PM_{2.5}$ and BC pollution, but their structure and organization throughout the urban environment can also influence local pollutant concentrations.

Urban structure patterns contributed less explanatory power for BC predictions as they did for $PM_{2.5}$ predictions. This may be explained in part BC being s a subset of $PM_{2.5}$. Chemically complex, $PM_{2.5}$ is inherently more abundant in the environment, as it has a greater variety of sources including vegetation, secondary aerosol formation from vehicular emissions (e.g. NO_x and SO_x) (Juda-Rezler et al., 2020), and suspension of crustal materials such as dust and soil (Querol et al., 2001). In contrast, BC is

 doi:10.20944/preprints202104.0588.v2

anthropogenic in nature, deriving from road transport (Diaz Resquin et al., 2018). These results support the idea that differences in three-dimensional urban structure alter the presence, abundance, and distribution of air pollution. Further understanding the role of vegetation and urban structure in air pollution dynamics can help strengthen the use of STURLA for urban planning.

Limitations

Though the sampling routes capture a sample of Philadelphia that is representative of the urban structure patterns prevalent in the city, the urban landscape can look quite different in other cities. As a result, some STURLA classes that are present or even abundant in other urban environments are not considered in these analyses. One such example is STURLA class *w*; though it is the sixth most common STURLA class in Philadelphia, we are unable to sample this class as it is impossible to drive through a cell containing only water. The accuracy of the prediction cannot be compared to measured values, as there are none; similar studies in the future should make appropriate adjustments to the experimental design to capture common classes that are otherwise inaccessible (i.e. classes without pavement). Though we include predictions and measurements for all classes with two or more observations, we do not test for significant differences between classes with fewer than 20 unique sampled cells, nor do we examine how the compositions of these classes influence pollutant concentrations. Infrequently sampled classes constitute a small fraction of the urban structure patterns present throughout Philadelphia. In the absence of further sampling it is difficult to accurately predict and characterize pollutant levels in these areas. Additionally, the use of STURLA is limited by the availability of up-to-date fine scale landcover and building height data; as the STURLA profile is based on data from 2018, it may not reflect changes in the Philadelphia's urban landscape that have occurred since then. Increased availability and accuracy of spatial data would make STURLA more effective in real time and would enable more accurate predictions.

Materials and Methods

Site Description

Philadelphia, Pennsylvania is the sixth-most populous city in the United States of America and the largest city in the state of Pennsylvania, with an estimated population of 1,584,138 residents in 2018. Philadelphia is a northeastern U.S. city defined by a dense urban core surrounded by predominantly low-rise residential and commercial districts, city parks, and industrial sectors. Two major rivers flow through the city: the Delaware River, which flows southward into the Delaware Bay and Atlantic Ocean, and the Schuylkill River, which flows southward through the western neighborhoods of Philadelphia. The southern and eastern parts of the city house heavy industry along both riverbanks, while large park areas are found in the western and northern areas of the city. For planning purposes, Philadelphia is divided into 18 different planning districts (Figure 1, Table A1).

Philadelphia STURLA

Preprints (www.preprints.org) | NOT PEER-REVIEWED | Posted: 5 May 2021 doi:10.20944/preprints202104.0588.v2

We created the STURLA classification for 2018 following the methodology outlined in Hamstead et al. (2016), Mitz et al. (2021), and Stewart et al. (2021). Fine scale landcover data and building height data were fused to create the underlying landcover dataset. A fishnet with cells of 120m^2\pixel was overlaid on the underlying landcover dataset. STURLA classifications for each cell were determined based on the presence of each landscape component present (see (Figure A1). Each letter in the STURLA code represents a different landscape component in the urban environment. Each class in a STURLA cell indicates a specific combination of different landscape components: trees (t), grass (g), bare soil (b), water (w), pavement (p), low-rise buildings (1 – 3 stories) (l), mid-rise buildings (4 – 9 stories) (m), and/or high-rise buildings (9+ stories) (h). Philadelphia contains 86 STURLA classes, although most of the city can be characterized by just a few classes; *tgpl* is by far the most common class, describing about 51.7% of Philadelphia. Other common classes include *tgplm*, *tgp*, *tgbpl*, *tgwp*, and *w.* The map in Figure 1 shows the spatial distribution of STURLA classes in Philadelphia. Whiting class composition, as the percent area of each landscape component, was calculated using the *Tabulate Area* tool in Arc Pro 2.4.

Sampling Description

A van, equipped with instrumentation measuring geolocation data (Trimble Juno 3B with Trimble R1 GNSS receivers), $PM_{2.5}$ concentrations (Grimm Portable Laser Aerosol Spectrometer, Model 11-C), and BC concentrations (MicroAeth MA200) was driven along two predetermined routes in Philadelphia. Sampling equipment was set up and calibrated as described in Cummings & Stewart et al. 2021. Data was captured at different temporal resolutions; GPS data was recorded at every one second interval, BC data was recorded at every five second interval, and PM data was recorded at every six second interval (Table A2).

Driving routes were determined using a stratified random sample of STURLA cells in order to ensure that a representative sample of Philadelphia's STURLA class distribution was captured during the sampling period (Figure A2). Specific points of interest such as United States Environmental Protection Agency (U.S. EPA) Toxics Release Inventory (TRI) sites, EPA air pollution monitoring station sites, the Philadelphia Water Department's green infrastructure sites, and census tracts with high rates of asthma were also considered in route development. An optimized ~483 km (300 mile) driving route that took STURLA class distribution and points of interest into account was generated using Network Analyst in ArcGIS 10.7.1. This optimized route was divided into two ~241.5 km (150 mile) segments in order to make the routes drivable within a day. Occasional road closures in Philadelphia created slight variability in the routes traveled from day to day.

Sampling occurred over a period of 12 days between June 27 and July 29, 2019; each route was sampled six times. Weather conditions during the sampling days were similar (Table A3). Sampling began between 6 – 7 AM on one of the two routes and continued until the entirety of the route was traveled. The daily average vehicle speed ranged from 23.3 – 29.9 km/hr.

Data Analysis

Air pollution and geolocation data were joined by time. For each day of data collection, air pollution data was spatially joined to Philadelphia's STURLA profile in

Preprints (www.preprints.org) | NOT PEER-REVIEWED | Posted: 5 May 2021 doi:10.20944/preprints202104.0588.v2

ArcGIS Pro 2.4; each pixel was assigned the value of the average concentration of all points that fell within it. All cells that contained at least one point were selected and summarized to obtain the average concentration for each STURLA class. The mean concentrations for each class on each day were averaged to determine an average daily mean concentration for each STURLA class for which at least 20 unique cells were sampled; classes that were sampled in fewer than 20 unique cells were summarized into an "other" class for which daily averages were calculated. Permutational t-tests (n= 10,000) from the "RVAidememoire" package in R were used to determine if differences in the daily mean air pollutant concentrations of STURLA classes were significant, as they take varying sample sizes into account (Hervé 2020). For each STRULA class sampled, the composition of an average cell was determined by finding the mean percentage of all landscape components within sampled cells belonging to a specific class. Differences in average STURLA class composition were evaluated using hierarchical clustering based on Bray-Curtis dissimilarities between classes. The clustering dendrogram (Figure 2) demonstrates compositional similarities between classes; classes with fewer branches separating them are more similar to each other than those with more branches separating them.

A supervised machine learning model, Random Forest Regression, was used to investigate the possible distribution of $PM_{2.5}$ and BC in areas not sampled based on measured concentrations and the STURLA landscape components in sampled areas. This method uses an ensemble of weak models that draw a random sample from the original dataset and splits them into a forest of decision trees, which helps to account for spatial autocorrelation and non-linear relationships more effectively than linear models (Oliveira, 2012). Using the "*caret"* package (Kuhn et al. 2008) in R (3.3.6) (Ihaka & Gentleman, 1996) data were split into 60% training and 40% validation sets that underwent 10-fold cross-validation. The model was trained using the average within-class percentage of landscape components for each class, and the mean pollutant concentration measured in that class (e.g. class *tgpl* is the supervised label attached to the mean landscape percentages for *tgpl* across Philadelphia). Root Mean Standard Error (RMSE) was used to assess model error. We define validation error as the ratio of predicted to measured concentrations. Variable importance is measured as the percent increase in RMSE by removing a variable from the model where once completed for each variable is ranked. Model predictions and results were joined by STURLA class and visualized using ArcMap 10.7.1.

Acknowledgments

We would like to thank Meghan Conway, Radley Reist, and Alexander Saad for their assistance in data collection. Financial support for this study was provided through National Science Foundation (NSF) grant #1832407.

References

1. United Nations, Department of Economic and Social Affairs, Population Division (2019). World Urbanization Prospects: The 2018 Revision. New York: United Nations.

2. World Health Organization (2018). 9 out of 10 people worldwide breathe polluted air, but more countries are taking action. News release, Geneva. https://www.who.int/news/item/02-05-2018-9-out-of-10-people-worldwide-breathe-polluted-air-but-more-countries-are-taking-action
3. Cohen, A. J., Brauer, M., Burnett, R., Anderson, H. R., Frostad, J., Estep, K., Balakrishnan, K., Brunekreef, B., Dandona, L., Dandona, R., Feigin, V., Freedman, G., Hubbell, B., Jobling, A., Kan, H., Knibbs, L., Liu, Y., Martin, R., Morawska, L., … Forouzanfar, M. H. (2017). Estimates and 25-year trends of the global burden of disease attributable to ambient air pollution: An analysis of data from the Global Burden of Diseases Study 2015. The Lancet, 389(10082), 1907–1918. https://doi.org/10.1016/S0140-6736(17)30505-6
4. Perlin, S. A., Sexton, K., & Wong, D. W. S. (1999). An examination of race and poverty for populations living near industrial sources of air pollution. Journal of Exposure Science & Environmental Epidemiology, 9(1), 29–48. https://doi.org/10.1038/sj.jea.7500024
5. Gray, S. C., Edwards, S. E., & Miranda, M. L. (2013). Race, socioeconomic status, and air pollution exposure in North Carolina. Environmental Research, 126, 152–158. https://doi.org/10.1016/j.envres.2013.06.005
6. Collins, T. W., Grineski, S. E., & Morales, D. X. (2017a). Sexual Orientation, Gender, and Environmental Injustice: Unequal Carcinogenic Air Pollution Risks in Greater Houston. Annals of the American Association of Geographers, 107(1), 72–92. https://doi.org/10.1080/24694452.2016.1218270
7. Collins, T. W., Grineski, S. E., & Morales, D. X. (2017b). Environmental injustice and sexual minority health disparities: A national study of inequitable health risks from air pollution among same-sex partners. Social Science & Medicine, 191, 38–47. https://doi.org/10.1016/j.socscimed.2017.08.040
8. Zhou, Z., Dionisio, K. L., Arku, R. E., Quaye, A., Hughes, A. F., Vallarino, J., Spengler, J. D., Hill, A., Agyei-Mensah, S., & Ezzati, M. (2011). Household and community poverty, biomass use, and air pollution in Accra, Ghana. Proceedings of the National Academy of Sciences, 108(27), 11028–11033. https://doi.org/10.1073/pnas.1019183108
9. Halonen, J. I., Lanki, T., Yli-Tuomi, T., Kulmala, M., Tiittanen, P., & Pekkanen, J. (2008). Urban air pollution, and asthma and COPD hospital emergency room visits. Thorax, 63(7), 635–641. https://doi.org/10.1136/thx.2007.091371
10. Anenberg, S. C., Henze, D. K., Tinney, V., Kinney, P. L., Raich W., Fann N., Malley, Chris S., Roman, H., Lamsal, L., Duncan B., Martin R. V., van Donkelaar, A., Brauer, M., Doherty, R., Jonson J. E., Davila, Y., Sudo Kengo, & Kuylenstierna, J. C. I. (2018). Estimates of the Global Burden of Ambient PM2.5, Ozone, and NO2 on Asthma Incidence and Emergency Room Visits. Environmental Health Perspectives, 126(10), 107004. https://doi.org/10.1289/EHP3766
11. Hamra, G. B., Guha, N., Cohen, A., Laden, F., Raaschou-Nielsen, O., Samet, J. M., Vineis, P., Forastiere, F., Saldiva, P., Yorifuji, T., & Loomis, D. (2014). Outdoor particulate matter exposure and lung cancer: A systematic review and meta-analysis. Environmental Health Perspectives, 122(9), 906–911. https://doi.org/10.1289/ehp/1408092
12. Pope III, C. A., Burnett, R. T., Thun, M. J., Calle, E. E., Krewski, D., Ito, K., & Thurston, G. D. (2002). Lung Cancer, Cardiopulmonary Mortality, and Long-term

Exposure to Fine Particulate Air Pollution. JAMA, 287(9), 1132–1141. https://doi.org/10.1001/jama.287.9.1132
13. Sørensen, M., Autrup, H., Hertel, O., Wallin, H., Knudsen, L. E., & Loft, S. (2003). Personal exposure to PM2.5 and biomarkers of DNA damage. Cancer Epidemiology, Biomarkers & Prevention: A Publication of the American Association for Cancer Research, Cosponsored by the American Society of Preventive Oncology, 12(3), 191–196.
14. Shi, Y., Zhao, T., Yang, X., Sun, B., Li, Y., Duan, J., & Sun, Z. (2019). PM2.5-induced alteration of DNA methylation and RNA-transcription are associated with inflammatory response and lung injury. Science of The Total Environment, 650, 908–921. https://doi.org/10.1016/j.scitotenv.2018.09.085
15. Baccarelli, A., Wright, R. O., Bollati, V., Tarantini, L., Litonjua, A. A., Suh, H. H., Zanobetti, A., Sparrow, D., Vokonas, P. S., & Schwartz, J. (2009). Rapid DNA Methylation Changes after Exposure to Traffic Particles. American Journal of Respiratory and Critical Care Medicine, 179(7), 572–578. https://doi.org/10.1164/rccm.200807-1097OC
16. Zelikoff, J. T., Chen, L. C., Cohen, M. D., Fang, K., Gordon, T., Li, Y., Nadziejko, C., & Schlesinger, R. B. (2003). Effects of Inhaled Ambient Particulate Matter on Pulmonary Antimicrobial Immune Defense. Inhalation Toxicology, 15(2), 131–150. https://doi.org/10.1080/08958370304478
17. Honda, A., Fukushima, W., Oishi, M., Tsuji, K., Sawahara, T., Hayashi, T., Kudo, H., Kashima, Y., Takahashi, K., Sasaki, H., Ueda, K., & Takano, H. (2017). Effects of Components of PM2.5 Collected in Japan on the Respiratory and Immune Systems. International Journal of Toxicology, 36(2), 153–164. https://doi.org/10.1177/1091581816682224
18. Stewart, J. D., Shakya, K. M., Bilinski, T., Wilson, J. W., Ravi, S., & Choi, C. S. (2020). Variation of near surface atmosphere microbial communities at an urban and a suburban site in Philadelphia, PA, USA. Science of The Total Environment, 724, 138353. https://doi.org/10.1016/j.scitotenv.2020.138353
19. Liu, H., Zhang, X., Zhang, H., Yao, X., Zhou, M., Wang, J., He, Z., Zhang, H., Lou, L., Mao, W., Zheng, P., & Hu, B. (2018). Effect of air pollution on the total bacteria and pathogenic bacteria in different sizes of particulate matter. Environmental Pollution, 233, 483–493. https://doi.org/10.1016/j.envpol.2017.10.070
20. Zhu, Y., Xie, J., Huang, F., & Cao, L. (2020). Association between short-term exposure to air pollution and COVID-19 infection: Evidence from China. Science of The Total Environment, 727, 138704. https://doi.org/10.1016/j.scitotenv.2020.138704
21. Dockery, D. W., Pope, C. A., Xu, X., Spengler, J. D., Ware, J. H., Fay, M. E., Ferris, B. G., & Speizer, F. E. (1993). An Association between Air Pollution and Mortality in Six U.S. Cities. New England Journal of Medicine, 329(24), 1753–1759. https://doi.org/10.1056/NEJM199312093292401
22. Paul, G., Nolen, J. E., Alexander, L., Bender, L. K., Vleet, V., Barrett, W., Jump, Z., Rappaport, S., Samet, J. M., Ballentine, N., Nimirowski, T., Innocenzi, L., Wojs, V., Lavelle, L., Clark, C., Fitzgerald, J., Eyer, A., Lacina, K., Macmunn, A., … Designs, O. (2019). State of the Air 2019. www.stateoftheair.org
23. Rabinovitch, N., Strand, M., & Gelfand, E. W. (2006). Particulate levels are associated with early asthma worsening in children with persistent disease.

American Journal of Respiratory and Critical Care Medicine, 173(10), 1098–1105. https://doi.org/10.1164/rccm.200509-1393OC
24. Shakya, K. M., Rupakheti, M., Aryal, K., & Peltier, R. E. (2016). Respiratory Effects of High Levels of Particulate Exposure in a Cohort of Traffic Police in Kathmandu, Nepal. Journal of Occupational and Environmental Medicine, 58(6), e218. https://doi.org/10.1097/JOM.0000000000000753
25. Hitzenberger, R., & Tohno, S. (2001). Comparison of black carbon (BC) aerosols in two urban areas – concentrations and size distributions. Atmospheric Environment, 35(12), 2153–2167. https://doi.org/10.1016/S1352-2310(00)00480-5
26. Cyrys, J., Heinrich, J., Hoek, G., Meliefste, K., Lewné, M., Gehring, U., Bellander, T., Fischer, P., Vliet, P. van, Brauer, M., Wichmann, H.-E., & Brunekreef, B. (2003). Comparison between different traffic-related particle indicators: Elemental carbon (EC), PM 2.5 mass, and absorbance. Journal of Exposure Science & Environmental Epidemiology, 13(2), 134–143. https://doi.org/10.1038/sj.jea.7500262
27. Targino, A. C., Gibson, M., Krecl, P., Rodrigues, M. V., Santos, M. M. D., & Corrêa, M. de P. (2016). Hotspots of black carbon and PM2.5 in an urban area and relationships to traffic characteristics. Environmental Pollution, 218, 475–486. https://doi.org/10.1016/j.envpol.2016.07.027
28. Eeftens, M., Beelen, R., de Hoogh, K., Bellander, T., Cesaroni, G., Cirach, M., Declercq, C., Dėdelė, A., Dons, E., de Nazelle, A., Dimakopoulou, K., Eriksen, K., Falq, G., Fischer, P., Galassi, C., Gražulevičienė, R., Heinrich, J., Hoffmann, B., Jerrett, M., … Hoek, G. (2012). Development of Land Use Regression Models for PM2.5, PM2.5 Absorbance, PM10 and PMcoarse in 20 European Study Areas; Results of the ESCAPE Project. Environmental Science & Technology, 46(20), 11195–11205. https://doi.org/10.1021/es301948k
29. Yuan, M., Song, Y., Huang, Y., Shen, H., & Li, T. (2019). Exploring the association between the built environment and remotely sensed PM2.5 concentrations in urban areas. Journal of Cleaner Production, 220, 1014–1023. https://doi.org/10.1016/j.jclepro.2019.02.236
30. Shakya, K. M., Kremer, P., Henderson, K., McMahon, M., Peltier, R. E., Bromberg, S., & Stewart, J. (2019). Mobile monitoring of air and noise pollution in Philadelphia neighborhoods during summer 2017. Environ. Pollut., 255(Pt 1), 113195–113195. https://doi.org/10.1016/j.envpol.2019.113195
31. Baldauf, R. W., Isakov, V., Deshmukh, P., Venkatram, A., Yang, B., & Zhang, K. M. (2016). Influence of solid noise barriers on near-road and on-road air quality. Atmospheric Environment, 129, 265–276. https://doi.org/10.1016/j.atmosenv.2016.01.025
32. Gallagher, J., Baldauf, R., Fuller, C. H., Kumar, P., Gill, L. W., & McNabola, A. (2015). Passive methods for improving air quality in the built environment: A review of porous and solid barriers. Atmospheric Environment, 120, 61–70. https://doi.org/10.1016/j.atmosenv.2015.08.075
33. Ng, W. Y., & Chau, C. K. (2012). Evaluating the role of vegetation on the ventilation performance in isolated deep street canyons. International Journal of Environment and Pollution, 50(1–4), 98–110. https://doi.org/10.1504/IJEP.2012.051184
34. Nemitz, E., Vieno, M., Carnell, E., Fitch, A., Steadman, C., Cryle, P., Holland, M., Morton, R. D., Hall, J., Mills, G., Hayes, F., Dickie, I., Carruthers, D., Fowler, D.,

Reis, S., & Jones, L. (2020). Potential and limitation of air pollution mitigation by vegetation and uncertainties of deposition-based evaluations. Philosophical Transactions of the Royal Society A: Mathematical, Physical and Engineering Sciences, 378(2183), 20190320. https://doi.org/10.1098/rsta.2019.0320

35. Brantley, H. L., Hagler, G. S. W., Kimbrough, E. S., Williams, R. W., Mukerjee, S., & Neas, L. M. (2014). Mobile air monitoring data-processing strategies and effects on spatial air pollution trends. Atmospheric Measurement Techniques, 7(7), 2169–2183. https://doi.org/10.5194/amt-7-2169-2014
36. Chen, L., Liu, C., Zou, R., Yang, M., & Zhang, Z. (2016). Experimental examination of effectiveness of vegetation as bio-filter of particulate matters in the urban environment. Environmental Pollution, 208, 198–208.
37. Eisenman, T. S., Churkina, G., Jariwala, S. P., Kumar, P., Lovasi, G. S., Pataki, D. E., Weinberger, K. R., & Whitlow, T. H. (2019). Urban trees, air quality, and asthma: An interdisciplinary review. Landscape and Urban Planning, 187(February), 47–59. https://doi.org/10.1016/j.landurbplan.2019.02.010
38. Xing, Y., & Brimblecombe, P. (2019). Role of vegetation in deposition and dispersion of air pollution in urban parks. Atmospheric Environment, 201(December 2018), 73–83. https://doi.org/10.1016/j.atmosenv.2018.12.027
39. Cadenasso, M. L., Pickett, S. T. A., & Schwarz, K. (2007). Spatial heterogeneity in urban ecosystems: Reconceptualizing landcover and a framework for classification. Frontiers in Ecology and the Environment, 5(2), 80–88. https://doi.org/10.1890/1540-9295(2007)5[80:SHIUER]2.0.CO;2
40. Hamstead, Z. A., Kremer, P., Larondelle, N., McPhearson, T., & Haase, D. (2016). Classification of the heterogeneous structure of urban landscapes (STURLA) as an indicator of landscape function applied to surface temperature in New York City. Ecological Indicators, 70, 574–585. https://doi.org/10.1016/j.ecolind.2015.10.014
41. Kremer, P., Larondelle, N., Zhang, Y., Pasles, E., & Haase, D. (2018). Within-class and neighborhood effects on the relationship between composite urban classes and surface temperature. Sustainability (Switzerland), 10(3). https://doi.org/10.3390/su10030645
42. Larondelle, N., Hamstead, Z. A., Kremer, P., Haase, D., & McPhearson, T. (2014). Applying a novel urban structure classification to compare the relationships of urban structure and surface temperature in Berlin and New York City. Applied Geography, 53, 427–437. https://doi.org/10.1016/j.apgeog.2014.07.004
43. Mitz, E., Kremer, P., Larondelle, N., & Stewart, J. (2020). Structure of Urban Landscape and Surface Temperature: A Case Study in Philadelphia, PA [Preprint]. Earth and Space Science Open Archive; Earth and Space Science Open Archive. https://doi.org/10.1002/essoar.10503832.1
44. Stewart, J. D., Kremer, P., Shakya, K. M., Conway, M., & Saad, A. (2021). Outdoor Atmospheric Microbial Diversity Is Associated With Urban Landscape Structure and Differs From Indoor-Transit Systems as Revealed by Mobile Monitoring and Three-Dimensional Spatial Analysis. Frontiers in Ecology and Evolution, 9. https://doi.org/10.3389/fevo.2021.620461
45. Abhijith, K. V., & Gokhale, S. (2015). Passive control potentials of trees and on-street parked cars in reduction of air pollution exposure in urban street canyons. Environmental Pollution, 204, 99–108. https://doi.org/10.1016/j.envpol.2015.04.013

46. Hagler, G. S. W., Lin, M. Y., Khlystov, A., Baldauf, R. W., Isakov, V., Faircloth, J., & Jackson, L. E. (2012). Field investigation of roadside vegetative and structural barrier impact on near-road ultrafine particle concentrations under a variety of wind conditions. Science of the Total Environment, 419, 7–15. https://doi.org/10.1016/j.scitotenv.2011.12.002
47. Apte, J. S., Messier, K. P., Gani, S., Brauer, M., Kirchstetter, T. W., Lunden, M. M., Marshall, J. D., Portier, C. J., Vermeulen, R. C. H., & Hamburg, S. P. (2017). High-Resolution Air Pollution Mapping with Google Street View Cars: Exploiting Big Data. Environmental Science & Technology, 51(12), 6999–7008. https://doi.org/10.1021/acs.est.7b00891
48. deSouza, P., Anjomshoaa, A., Duarte, F., Kahn, R., Kumar, P., & Ratti, C. (2020). Air quality monitoring using mobile low-cost sensors mounted on trash-trucks: Methods development and lessons learned. Sustainable Cities and Society, 60, 102239. https://doi.org/10.1016/j.scs.2020.102239
49. Deville Cavellin, L., Weichenthal, S., Tack, R., Ragettli, M. S., Smargiassi, A., & Hatzopoulou, M. (2016). Investigating the Use Of Portable Air Pollution Sensors to Capture the Spatial Variability Of Traffic-Related Air Pollution. Environmental Science & Technology, 50(1), 313–320. https://doi.org/10.1021/acs.est.5b04235
50. Sm, S. N., Reddy Yasa, P., Mv, N., Khadirnaikar, S., & Pooja Rani. (2019). Mobile monitoring of air pollution using low cost sensors to visualize spatio-temporal variation of pollutants at urban hotspots. Sustainable Cities and Society, 44, 520–535. https://doi.org/10.1016/j.scs.2018.10.006
51. Van Poppel, M., Peters, J., & Bleux, N. (2013). Methodology for setup and data processing of mobile air quality measurements to assess the spatial variability of concentrations in urban environments. Environmental Pollution, 183, 224–233. https://doi.org/10.1016/j.envpol.2013.02.020
52. Van den Bossche, J., Peters, J., Verwaeren, J., Botteldooren, D., Theunis, J., & De Baets, B. (2015). Mobile monitoring for mapping spatial variation in urban air quality: Development and validation of a methodology based on an extensive dataset. Atmospheric Environment, 105, 148–161. https://doi.org/10.1016/j.atmosenv.2015.01.017
53. Cummings, L. E., Stewart, J. D., Reist, R., Shakya, K. M., & Kremer, P. (2021). Mobile Monitoring of Air Pollution Reveals Spatial and Temporal Variation in an Urban Landscape. Frontiers in Built Environment, 7. https://doi.org/10.3389/fbuil.2021.648620
54. Hervé, M. (2021). RVAideMemoire: Testing and Plotting Procedures for Biostatistics (0.9-79) [Computer software]. https://CRAN.R-project.org/package=RVAideMemoire
55. Oliveira, S., Oehler, F., San-Miguel-Ayanz, J., Camia, A., & Pereira, J. M. C. (2012). Modeling spatial patterns of fire occurrence in Mediterranean Europe using Multiple Regression and Random Forest. Forest Ecology and Management, 275, 117–129. https://doi.org/10.1016/j.foreco.2012.03.003
56. Kuhn, M. (2008). Building Predictive Models in R Using the caret Package. Journal of Statistical Software, 28(1), 1–26. https://doi.org/10.18637/jss.v028.i05
57. Ihaka, R., & Gentleman, R. (1996). R: A Language for Data Analysis and Graphics. Journal of Computational and Graphical Statistics, 5(3), 299–314. https://doi.org/10.1080/10618600.1996.10474713
58. Aristodemou, E., Boganegra, L. M., Mottet, L., Pavlidis, D., Constantinou, A., Pain, C., Robins, A., & ApSimon, H. (2018). How tall buildings affect turbulent air

flows and dispersion of pollution within a neighbourhood. Environmental Pollution, 233, 782–796. https://doi.org/10.1016/j.envpol.2017.10.041
59. Zhang, A., Qi, Q., Jiang, L., Zhou, F., & Wang, J. (2013). Population Exposure to PM2.5 in the Urban Area of Beijing. PLOS ONE, 8(5), e63486. https://doi.org/10.1371/journal.pone.0063486
60. Zhou, S., & Lin, R. (2019). Spatial-temporal heterogeneity of air pollution: The relationship between built environment and on-road PM2.5 at micro scale. Transportation Research Part D: Transport and Environment, 76, 305–322. https://doi.org/10.1016/j.trd.2019.09.004
61. Nowak, D. J., Crane, D. E., & Stevens, J. C. (2006). Air pollution removal by urban trees and shrubs in the United States. Urban Forestry & Urban Greening, 4(3), 115–123. https://doi.org/10.1016/j.ufug.2006.01.007
62. Juda-Rezler, K., Reizer, M., Maciejewska, K., Błaszczak, B., & Klejnowski, K. (2020). Characterization of atmospheric PM2.5 sources at a Central European urban background site. Science of The Total Environment, 713, 136729. https://doi.org/10.1016/j.scitotenv.2020.136729
63. Querol, X., Alastuey, A., Rodriguez, S., Plana, F., Ruiz, C. R., Cots, N., Massagué, G., & Puig, O. (2001). PM10 and PM2.5 source apportionment in the Barcelona Metropolitan area, Catalonia, Spain. Atmospheric Environment, 35(36), 6407–6419. https://doi.org/10.1016/S1352-2310(01)00361-2
64. Diaz Resquin, M., Santágata, D., Gallardo, L., Gómez, D., Rössler, C., & Dawidowski, L. (2018). Local and remote black carbon sources in the Metropolitan Area of Buenos Aires. Atmospheric Environment, 182, 105–114. https://doi.org/10.1016/j.atmosenv.2018.03.018

Preprints (www.preprints.org) | NOT PEER-REVIEWED | Posted: 5 May 2021 doi:10.20944/preprints202104.0588.v2

Figures and Tables

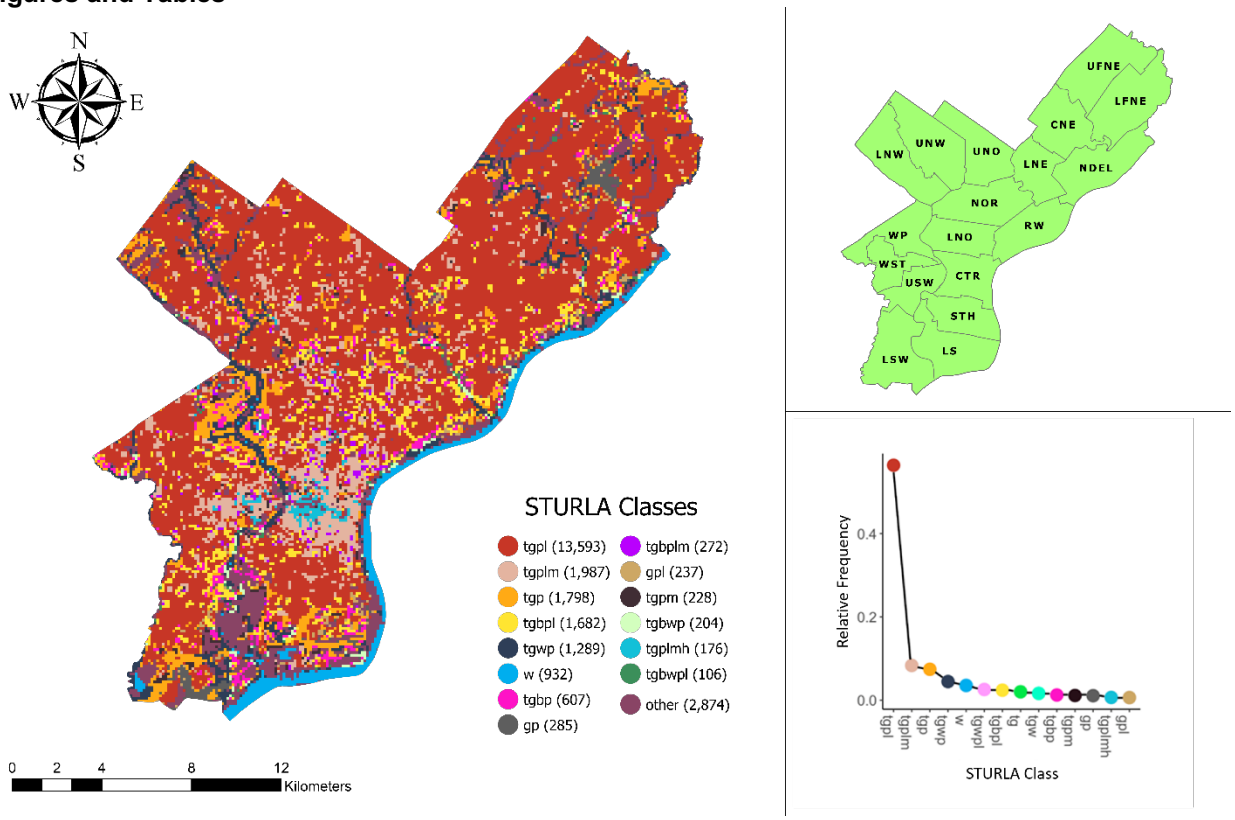

Figure 1. Map of STURLA classes in Philadelphia, Pennsylvania (left). Classes symbolized include the 14 most sampled classes, which make up 85.5% of Philadelphia; *w* is also included for representation of major waterways. The "other" class consists of the other 72 classes found throughout Philadelphia which, with water, characterize the remaining 14.5% of the city. Also included are Philadelphia's planning zones (top-right) and a ranked abundance plot (bottom-right) showing relative frequencies (%) of the 14 most abundant STURLA classes throughout Philadelphia.

Preprints (www.preprints.org) | NOT PEER-REVIEWED | Posted: 5 May 2021 doi:10.20944/preprints202104.0588.v2

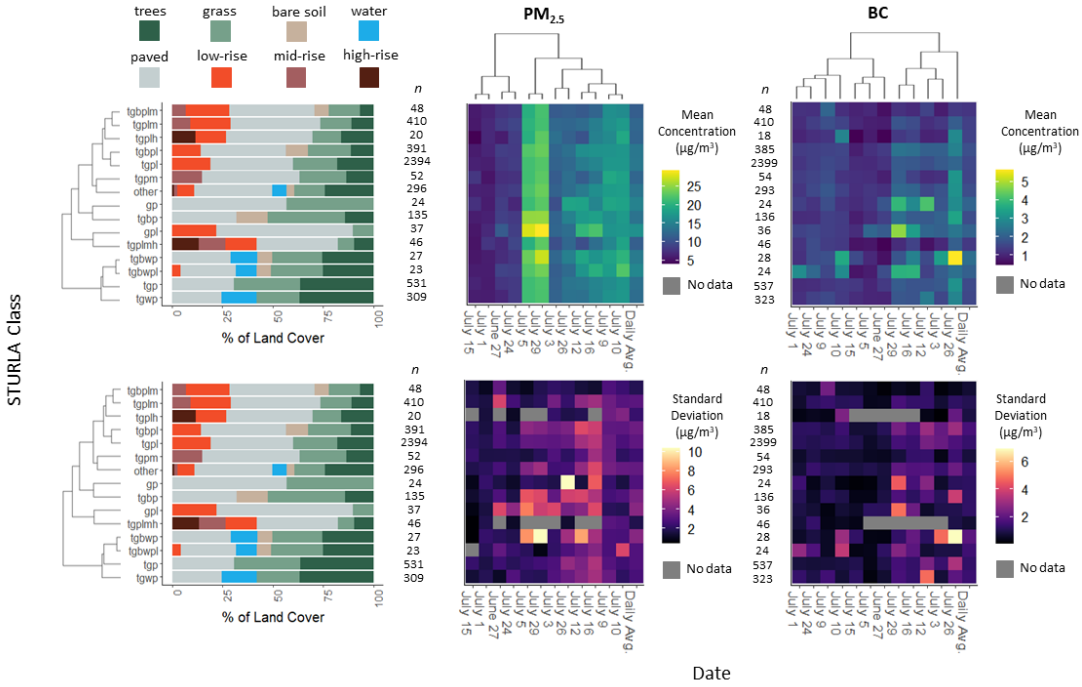

Figure 2. Composition of the average cell sampled for each class (left), sample sizes, and daily/overall means and standard deviations of measured $PM_{2.5}$ (middle) and BC (right) concentrations. Overall means are represented in the top heatmaps, while standard deviations are represented in the bottom heatmaps; darker colors (blue, purple) represent lower concentrations and lighter colors (yellow) represent higher concentrations. Dendrograms reflect similarities in pollutant concentrations between days (top) and STURLA class composition (left).

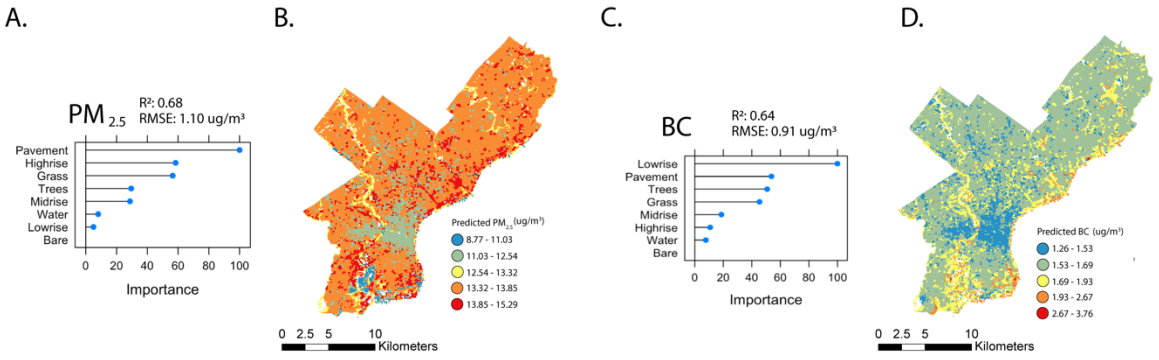

Preprints (www.preprints.org) | NOT PEER-REVIEWED | Posted: 5 May 2021 doi:10.20944/preprints202104.0588.v2

Figure 3. A. $PM_{2.5}$ Random Forest Regression variable importance, correlation coefficient (R^2) and error (RMSE). B. Predicted $PM_{2.5}$ concentrations by quantile. C. BC Random Forest Regression variable importance, correlation coefficient (R^2) and error (RMSE). D. Predicted BC concentrations by quantile